Magnetic properties of the doped spin-$\frac{1}{2}$ honeycomb-lattice compound $In_3Cu_2VO_9$

Y. J. Yan,[1] Z. Y. Li,[1] T. Zhang,[1] X. G. Luo,[1] G. J. Ye,[1] Z. J. Xiang,[1] P. Cheng,[1] L. J. Zou,[2] and X. H. Chen[1,*]

[1]*Hefei National Laboratory for Physical Science at Microscale and Department of Physics, University of Science and Technology of China, Hefei, Anhui 230026, People's Republic of China*

[2]*Institute of Solid State Physics, Chinese Academy of Sciences, Hefei, Anhui 230031, People's Republic of China*

(Received 8 June 2011; revised manuscript received 16 January 2012; published 9 February 2012)

We report magnetic properties in the Co- and Zn-doped spin-1/2 honeycomb-lattice compound $In_3Cu_2VO_9$. Magnetic susceptibility and specific heat experiments show no long-range ordering down to 2 K in $In_3Cu_2VO_9$. Analyses of electronic structures and states suggest that the ground state of undoped $In_3Cu_2VO_9$ is probably a Néel antiferromagnet (AFM). When Cu^{2+} ions are partially substituted by Co^{2+} ions, both the impurity potential scattering and magnetic scattering induced by the magnetic Co^{2+} ions enhance the three-dimensional character of the magnetic coupling and lead to an AFM long-range order. Replacement of Cu^{2+} with nonmagnetic Zn^{2+} ions weakens the AFM correlation between Cu^{2+} ions, leading to suppression of the AFM state.

DOI: 10.1103/PhysRevB.85.085102 PACS number(s): 75.40.Cx, 75.50.Ee, 71.27.+a

I. INTRODUCTION

Dimensionality and the spin magnitude S play important roles in the physical properties of interacting systems because quantum fluctuation is affected significantly by them. Quantum fluctuation enhanced both by geometric frustration and by spin frustration may destroy antiferromagnetic (AFM) order and yield a rich variety of ground states, novel excitations, and exotic behaviors that currently attract much attention. The magnetic properties of a solid reflect the arrangement of the magnetic ions in its crystal structure. Low-dimensional AFMs exhibit a variety of ground states depending on the spin number and the spin configuration.[1] In the first few years following the discovery of high-temperature superconductivity by Bednorz and Müller,[2] $S = 1/2$ two-dimensional (2D) systems on a square lattice have been in the center of attention. The honeycomb-lattice Heisenberg antiferromagnet $Bi_3Mn_4O_{12}(NO_3)$ revealed a novel spin-liquid-like behavior down to low temperature, which is ascribed to the frustration effect due to the competition between the AFM nearest- and next-nearest-neighbor interactions J_1 and J_2;[3–5] since its discovery growing interest has arisen in low-dimensional magnets with a honeycomb lattice. The honeycomb lattice is a loosely coupled lattice with only three nearest-neighbor sites; it might be susceptible to the fluctuation effect caused by frustration, and its ordering properties are of special interest. Experimentally there are only a few examples of materials where the electron spins are located in a two-dimensional honeycomb lattice. However, diverse phenomena, such as the spin-glass[6,7] and spin-liquid states,[3] Kosterlitz-Thouless transitions,[8,9] and superconductivity,[10,11] have been reported.

Recently, a complex transition-metal oxide, $In_3Cu_2VO_9$, was suggested as a possible candidate for the realization of the $S = 1/2$ honeycomb lattice.[12] $In_3Cu_2VO_9$ was previously reported to crystallize in the hexagonal space group $P6_3/mmc$, consisting of alternating layers of [InO_6] octahedra, and Cu^{2+} and V^{5+} ions in a trigonal-bipyramidal coordination.[12] The Cu^{2+} ($3d^9$, $S = 1/2$) ions were proposed to be arranged in a 2D network of hexagons with the nonmagnetic V^{5+} ($3d^0$) ions in the center of each hexagon. A later structural neutron diffraction study revealed a structural $\{V_1Cu_{6/3}\}$ order in the hexagonal planes with the finite correlation length $\xi_{st} \sim 300$ Å, and that these structural domains are randomly arranged along the c axis.[13] The static susceptibility $\chi(T)$ shows a broad maximum at $T_0 \sim 180$ K, which is a characteristic feature of a low-dimensional antiferromagnet, and passes through a kink at $T_1 \sim 38$ K followed by a peak at $T_2 \sim 28$ K. The anomaly at T_2 previously identified with the transition to the long-range-ordered state[12] has been tentatively assigned to glasslike order of unsaturated spins in domain boundaries by Möller *et al.*[13] Although no 3D magnetic peaks are seen in the neutron-scattering data and there is no indication of a phase transition in the specific heat, Yehia *et al.*[14] claimed that strong experimental evidence for the formation of a Néel-type collinear AFM spin structure was found in the $S = 1/2$ honeycomb plane at temperatures below ~20 K by electron spin resonance and nuclear magnetic resonance.

To obtain insights into the nature of the puzzling properties of the ground state of the spin-1/2 honeycomb-lattice compound $In_3Cu_2VO_9$, we have investigated the magnetic properties of the Co- and Zn-doped compound. Analyses of the electronic structures and states suggest that the ground state of undoped $In_3Cu_2VO_9$ is probably a Néel AFM. When the Cu^{2+} ions are partially substituted by Co^{2+} ions, the low-dimensional AFM at 180 K is quickly destroyed, while a long-rang AFM transition can be observed in the temperature range from 50 to 80 K, depending on Co concentration. When Zn is doped into the Cu sites, the low-dimensional AFM and the anomaly at T_2 in the magnetic susceptibility are gradually suppressed and completely disappear at heavy Zn doping level.

II. MATERIAL PREPARATION AND METHODS

$In_3Cu_2VO_9$ polycrystalline pellets were synthesized by a conventional solid-state technique. The starting materials In_2O_3, CuO, and V_2O_5 in a molar ratio of 3:4:1 were thoroughly ground and pressed into pellets. They were then heated at 1173 K in air for 5 days with several intermediate grindings and pelleting. $In_3Cu_{2-x}Co_xVO_9$ or $In_3Cu_{2-x}Zn_xVO_9$ was synthesized using In_2O_3, CuO, V_2O_5, and Co_3O_4, or ZnO as starting materials. The raw materials were accurately weighed according to the stoichiometric ratio of the chemical formulas, and then synthesized using a procedure similar to that for $In_3Cu_2VO_9$.

The samples were characterized by x-ray diffraction (XRD) using a Rigaku D/max-A x-ray diffractometer with Cu $K\alpha$

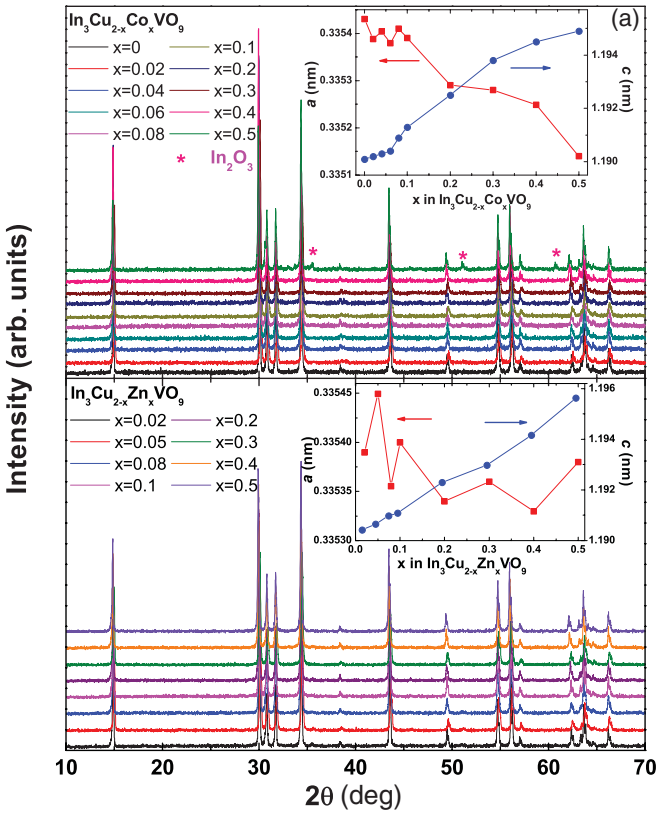

FIG. 1. (Color online) Powder x-ray diffraction patterns at room temperature for polycrystalline samples: (a) $In_3Cu_{2-x}Co_xVO_9$; (b) $In_3Cu_{2-x}Zn_xVO_9$. The peaks marked with stars reveal the existence of the impurity phase In_2O_3. Insets show the doping dependence of *a*- and *c*-axis lattice parameters.

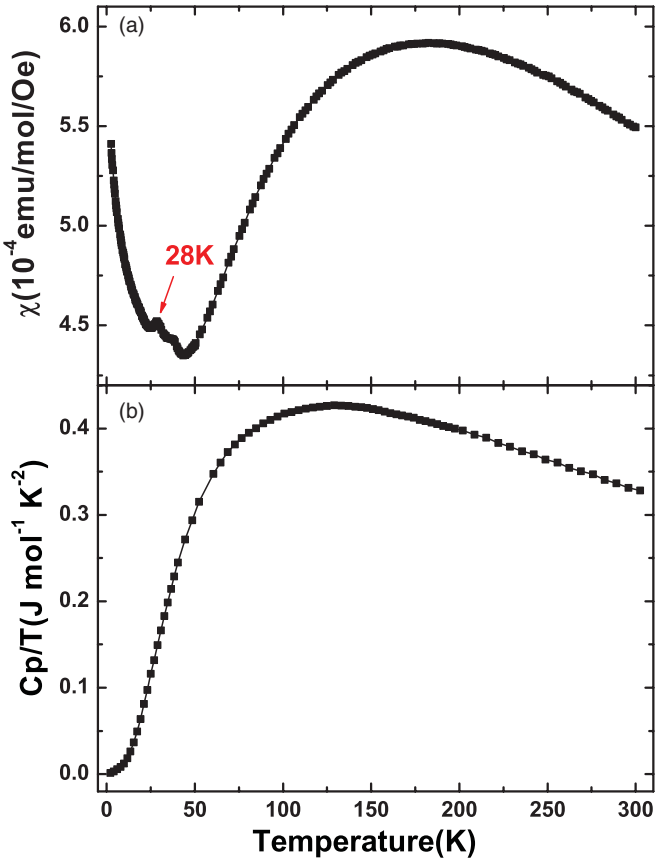

FIG. 2. (Color online) (a) The static magnetic susceptibility of $In_3Cu_2VO_9$ in the temperature range from 2 to 300 K under a magnetic field of 1 T. (b) Temperature dependence of specific heat divided by T for $In_3Cu_2VO_9$.

radiation in the range of 10°–70° with a step of 0.02° at room temperature. Sample purity was checked by powder x-ray diffraction, which showed no impurity peaks except for the sample $In_3Cu_{1.5}Co_{0.5}VO_9$ in which a trace of In_2O_3 was observed. Magnetic susceptibility was measured using a vibrating-sample magnetometer. Specific-heat measurements were carried out from 2 K to room temperature using a Quantum Design physical property measurement system.

III. RESULTS AND DISCUSSION

Figures 1(a) and 1(b) show the powder x-ray diffraction patterns for $In_3Cu_{2-x}Co_xVO_9$ and $In_3Cu_{2-x}Zn_xVO_9$ polycrystalline samples, respectively. It is found that all the peaks in the XRD diffraction pattern can be well indexed to a hexagonal structure. As seen in the inset of Fig. 1(a), with increasing Co doping concentration, the lattice parameter in the *a* direction decreases monotonically while that in the *c* direction increases monotonically. In the $In_3Cu_{2-x}Zn_xVO_9$ system, the lattice parameter in the *c* direction increases with increasing Zn doping concentration, while the change of the lattice parameter in the *a* direction is not obvious because it is smaller than 0.0001 nm.

The static magnetic susceptibility $\chi(T)$ for $In_3Cu_2VO_9$ was measured in a magnetic field of 1 T. The temperature dependence of χ for $In_3Cu_2VO_9$ reveals a broad maximum at $T_0 \sim 180$ K, which is a characteristic feature of low-dimensional antiferromagnets, passes through a kink at $T_1 \sim 38$ K followed by a peak at $T_2 \sim 28$ K, and shows a Curie-like upturn at lower temperatures [as seen in Fig. 2(a)]. The temperature dependence of the specific heat divided by T for $In_3Cu_2VO_9$ is shown in Fig. 2(b); no signature for a magnetic transition above 2 K is observed. These results are consistent with previous reports.[13–15] The experimental data for both the specific heat and magnetic susceptibility do not exhibit long-range AFM ordering, while strong experimental evidence for the formation of the Néel-type collinear AFM spin structure was found by ESR and NMR in the $S = 1/2$ honeycomb plane at temperatures below ~20 K.[14] These behaviors have also been observed in a $PbTiO_3$-type perovskite with a large tetragonal distortion, $PbVO_3$, which is a two-dimensional antiferromagnet with a long-range-ordering temperature of 43–50 K.[16,17] To further confirm the ground state of $In_3Cu_2VO_9$, we performed first-principle calculations on this material.

Theoretically, Clark *et al.*[18] showed that in a honeycomb J_1-J_2 Heisenberg model, when the ratio of the next-nearest-neighbor (NNN) spin coupling J_2 to the nearest-neighbor (NN) coupling J_1 is smaller than 0.08 or larger than 0.3, the honeycomb system exhibits long-range Néel AFM order or quantum dimer order; meanwhile, when $0.08 < J_2/J_1 < 0.3$, strong spin frustration and spin fluctuations can stabilize a spin-liquid phase in a Heisenberg insulator. Thus if we could determine the microscopic interaction parameters in undoped $In_3Cu_2VO_9$, the ground state of the parent phase would be completely

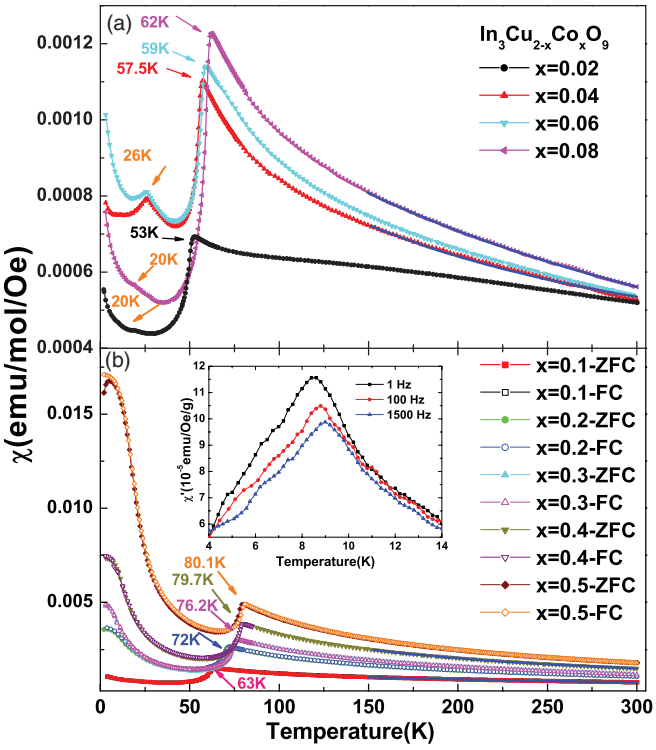

FIG. 3. (Color online) Temperature dependence of the magnetic susceptibility for $In_3Cu_{2-x}Co_xVO_9$ polycrystalline samples in the temperature range from 2 to 300 K under a magnetic field of 1 T. Arrows denote the occurrence temperatures of the long-range AFM ordering and the peaklike anomaly. The inset shows the real part of the ac magnetic susceptibility for $In_3Cu_{1.6}Co_{0.4}VO_9$ under different frequencies of 1, 100, and 1500 Hz with the ac magnetic field of 3.8 Oe at low temperature. The blue solid lines are fitting curves as described in the text.

determined. We find that $In_3Cu_2VO_9$ is a charge-transfer insulator with an energy gap of 1.6 eV, which is confirmed by the generalized gradient approximation (GGA) + U simulation done by Guo *et al.*[19] Well-localized magnetic moments in honeycomb-lattice copper spins with $S = 1/2$ form a hexagonal net in the Cu-V-O layer, showing that the low-energy magnetic properties of $In_3Cu_2VO_9$ can be described by a honeycomb Heisenberg model. The analyses of electronic structures and states[19] give the tight-binding parameters in the undoped phase, showing that the intralayer NN hopping integral between Cu $3d$ electrons in the $d_{3z^2-r^2}$ orbit, t_1, is about -0.18 eV, and the intralayer NNN hopping integral is quite large, $t_2 = -0.027$ eV; the interlayer hopping integral $t_z = -0.043$ eV, which is comparable with the NNN hopping integral. Considering the large on-site Coulomb interaction in Cu ions, $U \approx 8$ eV, we obtain the spin-spin coupling strengths as $J_1 = 17.5$ meV for the intralayer NN Cu spins, $J_2 = 0.4$ meV for the intralayer NNN Cu spins, and $J_z = 0.5$ meV for the interlayer NN Cu spins. This gives $J_2/J_1 = 0.02$, which is significantly smaller than the lower limit of the criteria for the occurrence of a spin-liquid state.[18] Therefore, we conclude that the ground state of undoped $In_3Cu_2VO_9$ is probably a Néel AFM. Furthermore, the ratio $J_z/J_1 = 0.03$, showing that the magnetic couplings are highly anisotropic and suggesting that $In_3Cu_2VO_9$ is a rather strong quasi-two-dimensional AFM.

The temperature dependence of the static magnetic susceptibility for the $In_3Cu_{2-x}Co_xVO_9$ samples is shown in Figs. 3(a) and 3(b). The Weiss temperature is positive, which is obtained by fitting the magnetic susceptibility between 150 and 300 K to the Curie-Weiss law $\chi = C/(T-\theta) + \chi_0$ (C is the Curie constant, θ is the Weiss temperature, and χ_0 is the temperature-independent term), indicating an AFM interaction between divalent transition-metal ions (M^{2+}). The effective magnetic moment of the transition-metal ions M^{2+} increases from $1.29\mu_B$ for $In_3Cu_{1.96}Co_{0.04}VO_9$ to $2.32\mu_B$ for $In_3Cu_{1.6}Co_{0.4}VO_9$. The spin quantum number of Co^{2+} ions is 3/2. It is obvious that the effective magnetic moments in this system are smaller than the intrinsic magnetic moments of magnetic ions. The AFM spin fluctuations arising from the low dimensionality ($D = 2$) and small spin ($S = 1/2$) can considerably suppress the magnetic moments and lead to smaller effective magnetic moments in Cu spins. When the Cu^{2+} ions are partially substituted by Co^{2+} ions, the low-dimensional AFM at about 180 K is quickly destroyed, while a long-range AFM transition can be observed in the temperature range from 50 to 80 K (marked by arrows in Fig. 3), depending on the Co concentration. The transition temperature T_N of the long-range AFM order increases with Co concentration, tending a finite temperature of about 80 K when x is larger than 0.4. Meanwhile, one notes that the magnitude of the magnetization increases with increasing Co concentration due to the larger intrinsic magnetic moment of Co^{2+} than Cu^{2+}. The occurrence of the long-range AFM order in Co-doped samples may be attributed to the enhancement of 3D AFM character through Co doping. When the Co doping level is less than 0.08, there is a peaklike anomaly with a Curie-like upturn below 40 K. The anomaly is suppressed and disappears when the Co doping level is more than 0.08. As shown in Fig. 3(b), a trace of a spin-glass-like contribution with $T_g < 10$ K is observed. The real part of the ac magnetic susceptibility for $In_3Cu_{1.6}Co_{0.4}VO_9$ under different frequencies of 1, 100, and 1500 Hz with an ac magnetic field of 3.8 Oe is shown in the inset of Fig. 3(b). The real part of the ac magnetic susceptibility

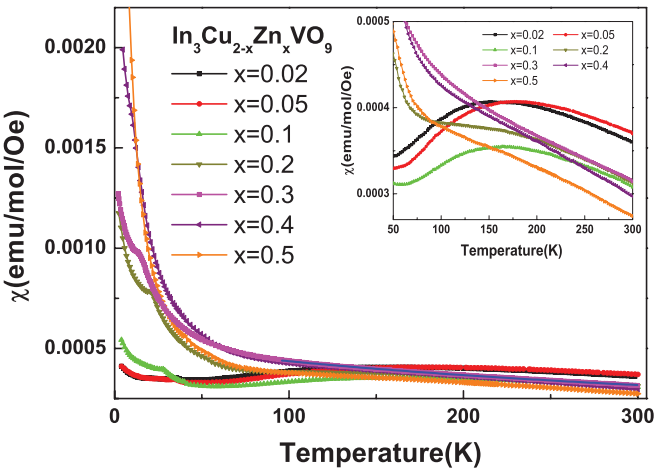

FIG. 4. (Color online) Temperature dependence of the magnetic susceptibility for $In_3Cu_{2-x}Zn_xVO_9$ polycrystalline samples in the temperature range from 2 to 300 K under a magnetic field of 1 T. The inset shows an enlargement of the magnetic susceptibility $\chi(T)$ above 50 K. The blue solid lines are fitting curves as described in the text.

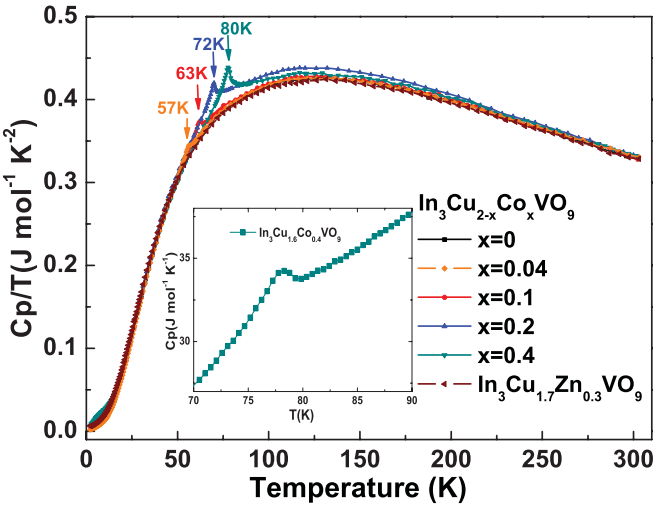

FIG. 5. (Color online) Temperature dependence of the specific heat divided by T for samples of the $In_3Cu_{2-x}Co_xVO_9$ and $In_3Cu_{2-x}Zn_xVO_9$ systems. The inset shows the anomaly in the specific heat for $In_3Cu_{1.6}Co_{0.4}VO_9$ around the phase transition.

shows a peak around 9 K, and it shifts to higher temperature with increasing frequency. This behavior strongly supports the glassy nature of the magnetic state in this compound.

In order to compare with Co doping, we tried to dope nonmagnetic Zn^{2+} ions into Cu^{2+} sites. Figure 4 shows the temperature dependence of the static magnetic susceptibility of the $In_3Cu_{2-x}Zn_xVO_9$ samples. On replacement of Cu^{2+} with Zn^{2+} ions, both the intensity and the temperature of the peaklike anomaly are suppressed with increasing Zn concentration, and the anomaly is destroyed when the Zn concentration is more than 0.3. As seen in the inset of Fig. 4, the broad hump at T_0 is notable when the Zn concentration x is less than 0.2, tends to be suppressed with higher Zn doping, and disappears when $x \geqslant 0.3$. The Weiss temperature and effective magnetic moment for $x = 0.3,0.4,0.5$ samples are 19.6,2.3,1.2 K and $0.30\mu_B$,$0.29\mu_B$,$0.26\mu_B$, respectively. They are much smaller than those of Co-doped samples. Therefore, with increasing Zn^{2+} doping concentration, the AFM correlation strength between Cu^{2+} ions is weakened, leading to the suppression of AFM ordering. Once $x \geqslant 0.3$, the strength of the correlation between Cu^{2+} ions is not large enough to form AFM order, and a paramagnetic state is observed.

Figure 5 shows the specific heat divided by T for some samples of these two systems. A λ-shape-like jump is observed in all the Co-doped samples from 50 to 80 K, which is ascribed to a long-range AFM transition. For $In_3Cu_{1.7}Zn_{0.3}VO_9$ without low-dimensional AFM behavior, no anomaly is observed around the temperature corresponding to the peak at about T_2 of the magnetic susceptibility. Therefore, the peaklike anomaly of the magnetic susceptibility is not associated with long-range ordering. A neutron diffraction study revealed a structural $\{V_1Cu_{6/3}\}$ order in the hexagonal planes with a finite correlation length $\xi_{st} \sim 300$ Å and these structural domains are randomly arranged along the c axis.[13] The peaklike anomalies in the magnetic susceptibility around 28 K have been tentatively assigned to glasslike order of unsaturated spins in domain boundaries by Möller *et al.*[13] Since we do not observe any abnormal specific heat around 28 K, therefore, we consider that the peaklike anomaly of magnetic susceptibility around 28 K is not associated with long-range ordering and might arise from unsaturated spins in domain boundaries.

After substituting Cu^{2+} with Co^{2+} in $In_3Cu_2VO_9$, one expects that the location of the Co^{2+} ions is random. Obviously, both impurity potential scattering and magnetic scattering induced by Co^{2+} ions ($S = 3/2$) enhance the AFM long-range correlation and lead to an AFM phase transition in specific heat and magnetic susceptibility. Such a scenario can address various temperature-dependent properties that we observed in experiments over a wide doping range, for example, the various AFM-paramagnetic phase transition peak as observed in the specific heat and magnetic susceptibility in many doped samples. The AFM correlation length of magnetic M^{2+} ions increases with increasing Co^{2+} concentration, leading to higher AFM transition temperatures. Meanwhile, by replacing Cu^{2+} with nonmagnetic Zn^{2+} ions, which are also randomly located, the AFM correlation between Cu^{2+} ions is destroyed, leading to the suppression of the low-dimensional AFM.

IV. CONCLUSION

In summary, we successfully synthesized the Co- and Zn-doped spin-1/2 honeycomb-lattice compounds $In_3Cu_{2-x}Co_xVO_9$ ($0 \leqslant x \leqslant 0.5$) and $In_3Cu_{2-x}Zn_xVO_9$ ($0 \leqslant x \leqslant 0.5$) and studied their magnetic properties. The magnetic susceptibility and specific heat experiments of $In_3Cu_2VO_9$ show no long-range ordering down to 2 K. Analyses of the electronic structures and states suggest that the ground state of undoped $In_3Cu_2VO_9$ is probably a Néel AFM. When the Cu^{2+} ions are partially substituted by Co^{2+} ions, the low-dimensional AFM at about 180 K is quickly destroyed, while a long-range AFM transition is observed in the temperature range from 50 to 80 K, depending on Co concentration. Both impurity potential scattering and magnetic scattering induced by magnetic Co^{2+} ions enhance the three-dimensional AFM long-range correlation. When Cu^{2+} ions are replaced with nonmagnetic Zn^{2+} ions, the AFM correlation between Cu^{2+} ions is weakened, leading to suppression of the AFM order.

ACKNOWLEDGMENTS

This work is supported by National Basic Research Program of China (973 Program, Grant No. 2012CB922002 and No. 2011CB00101), the National Natural Science Foundation of China (Grant No. 11190020 and No. 51021091), the Ministry of Science and Technology of China, and Chinese Academy of Sciences.

*chenxh@ustc.edu.cn

[1] A. P. Ramirez, Annu. Rev. Mater. Sci. **24**, 453 (1994).
[2] J. G. Bednorz and K. A. Müller, Z. Phys. B **64**, 189 (1986).
[3] O. Smirnova, M. Azuma, N. Kumada, Y. Kusano, M. Matsuda, Y. Shimakawa, T. Takei, Y. Yonesaki, and N. Kinomura, J. Am. Chem. Soc. **131**, 8313 (2009).

[4]M. Matsuda, M. Azuma, M. Tokunaga, Y. Shimakawa, and N. Kumada, Phys. Rev. Lett. **105**, 187201 (2010).
[5]S. Okumura, H. Kawamura, T. Okubo, and Y. Motome, J. Phys. Soc. Jpn. **79**, 114705 (2010).
[6]M. Bieringer, J. E. Greedan, and G. M. Luke, Phys. Rev. B **62**, 6521 (2000).
[7]N. Rogado, Q. Huang, J. W. Lynn, A. P. Ramirez, D. Huse, and R. J. Cava, Phys. Rev. B **65**, 144443 (2002).
[8]H. M. Rønnow, A. R. Wildes, and S. T. Bramwell, Physica B **276**, 676 (2000).
[9]M. Heinrich, H.-A. Krug von Nidda, A. Loidl, N. Rogado, and R. J. Cava, Phys. Rev. Lett. **91**, 137601 (2003).
[10]S. Shamoto, T. Kato, Y. Ono, Y. Miyazaki, K. Ohoyama, M. Ohashi, Y. Yamaguchi, and T. Kajitani, Physica C **306**, 7 (1998).
[11]R. Weht, A. Filipetti, and W. E. Pickett, Europhys. Lett. **48**, 320 (1999).
[12]V. Kataev, A. Möller, U. Löw, W. Jung, N. Schittner, M. Kriener, and A. Freimuth, J. Magn. Magn. Mater. **290**, 310 (2005).
[13]A. Möller, U. Löw, T. Taetz, M. Kriener, G. André, F. Damay, O. Heyer, M. Braden, and J. A. Mydosh, Phys. Rev. B **78**, 024420 (2008).
[14]M. Yehia, E. Vavilova, A. Möller, T. Taetz, U. Löw, R. Klingeler, V. Kataev, and B. Büchner, Phys. Rev. B **81**, 060414(R) (2010).
[15]Y. Fujii, D. Takahashi, Y. Kubo, H. Kikuchi, A. Matsuo, K. Kindo, S. Okubo, and H. Ohta, J. Phys.: Conf. Ser. **200**, 022010 (2010).
[16]K. Oka, I. Yamada, M. Azuma, S. Takeshita, K. H. Satoh, A. Koda, R. Kadono, M. Takano, and Y. Shimakawa, Inorg. Chem. **47**, 7355 (2008).
[17]A. A. Tsirlin, A. A. Belik, R. V. Shpanchenko, E. V. Antipov, E. T. Muromachi, and H. Rosner, Phys. Rev. B **77**, 092402 (2008).
[18]B. K. Clark, D. A. Abanin, and S. L. Sondhi, Phys. Rev. Lett. **107**, 087204 (2011).
[19]Y. Guo, G. R. Zhang, Liang-Jian Zou, Zhi Zeng, and H. Q. Lin (unpublished).